

Fabrication of Novel Three-Dimensional Microstructures by the Anisotropic Etching of (100) and (110) Silicon

ERNEST BASSOUS

Abstract—The anisotropic etching of single crystal silicon of (100) and (110) orientation in a solution of pyrocatechol, ethylene diamine, and water is reviewed and the fabrication of three novel types of microstructures is described in detail. Controlled etching of Si, which is required to fabricate devices with a predictable geometry depends on an accurately oriented, defect-free substrate, a well-defined and aligned pattern geometry, and rigorously clean etching conditions. Conventional IC processing methods were used to fabricate: 1) a high-precision circular orifice in a thin p^+ Si membrane for use as an ink jet nozzle, 2) a multisocket miniature electrical connector with octahedral cavities suitable for cryogenic applications, and 3) multichannel arrays in (100) and (110) Si useful in various applications, e.g., charge electrodes, physical masks, and optical devices. To make some of these structures, a novel bonding technique to fuse silicon wafers with phosphosilicate glass films was developed.

delineated in an appropriate masking film on the substrate surface, and c) the control exercised over the anisotropic etching conditions. These factors will be discussed first, followed by a description of the fabrication of the ink jet nozzle, the electrical connector, and last, the multichannel arrays.

ETCHING BEHAVIOR OF (100) AND (110) ORIENTED SILICON

Substrate

The etch rate of single crystal Si in an anisotropic etchant such as P-ED solution, varies with the crystallographic orientation of the substrate, and decreases, generally, in the order (100) > (110) > (111). Cavities and mesas etched in Si wafers are bounded by sidewalls which represent the fastest and slowest etching planes of the crystal. To predict the geometry of these structures, in (100) Si for example, it is necessary to know the etch rates $R_{(100)}$ and $R_{(111)}$ of the (100) and (111) planes, respectively. In practice, the anisotropic etch rate ratio $R_{(100)}/R_{(111)}$ is first determined experimentally for a given device structure and this ratio is then used to establish device design parameters. A high and uniform value of $R_{(100)}/R_{(111)}$ enables the fabrication of small-geometry and high-density microstructures.

High-quality Si wafers of (100) orientation, accurately oriented within $\pm 1^\circ$ of their crystal axes, are readily available commercially in a wide range of diameter, thickness, surface finish, conductivity type, and resistivity. Wafers of (110) orientation are often of questionable quality and are not readily available due to their limited use in industry. Thermally grown SiO_2 was used almost exclusively as an etch mask because it is readily formed as a thin, uniform, defect-free film on clean Si surfaces regardless of the shape of the Si structure. SiO_2 is compatible with most device fabrication processes and its etch rate in P-ED is extremely low. SiO_2 films grown at 900–1100°C in steam, 0.5 to 2.0 μm thick were generally used in most processes.

The geometry of holes etched through openings in a surface oxide film is a function of the orientation of the Si substrate, the geometry of the opening, its alignment relative to the wafer's crystal axes, and the duration of etching. Fig. 1 illustrates the shape of three holes anisotropically etched in (100) Si through openings of different geometry in a surface masking film. After sufficient etching has occurred, the hole in the Si surface is a rectangle which encloses the opening in the surface masking film. The etched holes are bounded by four convergent {111} planes each of which makes an angle of 54.74°

INTRODUCTION

ANISOTROPIC etching of single crystal silicon resulting from the differential etch rate of its crystallographic planes has been used to fabricate a variety of active and passive, three-dimensional device structures which include X-ray masks [1]–[6], optical waveguides [7]–[9], high-resolution patterns [10]–[14], nozzles [15]–[18], microtools [19], diodes [20], [21], bipolar and MOSFET circuits [22]–[27], electromechanical [28] and micromechanical [29], [30] devices. Preferential and nonpreferential etching techniques have also been used to fabricate a wide variety of surface structured devices [31]–[33]. In this paper the anisotropic etching of (100) and (110) oriented single crystal silicon is reviewed, and the fabrication of three types of novel device structures in (100) and (110) Si is described. The devices are 1) a high-precision nozzle useful in ink jet printing, 2) a multisocket miniature electrical connector for use at cryogenic temperatures, 3) multichannel array structures useful in a variety of applications. The last two types of devices were fabricated by employing a novel bonding technique which is compatible with silicon IC (integrated circuit) processing methods. The anisotropic etching solution which was used in fabricating the structures was first reported by Finne and Klein [34] and contained pyrocatechol $\text{C}_6\text{H}_4(\text{OH})_2$, (P), ethylene diamine $\text{NH}_2(\text{CH}_2)_2\text{NH}_2$, (ED) and water.

The fabrication of precision three-dimensional microstructures by the anisotropic etching of Si is influenced by the following factors: a) the crystallographic perfection of the substrate, b) the geometry of the surface pattern which is

Manuscript received February 6, 1978; revised May 8, 1978.
The author is with IBM Thomas J. Watson Research Center, Yorktown Heights, NY 10598.

P-ED Etchant

Uniform and controlled etching was obtained with an etchant of the following composition: 4 m % (mol percent) pyrocatechol, 46.4 m % ethylene diamine, and 49.4 m % water. The solution was used at its boiling point $118 \pm 1^\circ\text{C}$, in a nonoxidizing atmosphere, and its composition was maintained constant by means of a reflux condenser system [35]. The etch rates of the {100}, {110}, and {111} planes in P-ED are 50, 30, and $1 \mu\text{m/h}$, respectively, based on measurements of etched cavities in (100) and (110) Si substrates. The etch rates of thermally grown SiO_2 and chemically vapor deposited Si_3N_4 films are 150 and 80 \AA/h , respectively. The low etch rate of SiO_2 in this etchant is a distinct advantage in the fabrication of devices which require prolonged etching.

Due to the high etch selectivity of P-ED, residues or contaminants adhering to clean Si surfaces cause local masking and consequently nonuniform etching. Rigorously clean Si surfaces were thus necessary for the controlled etching of precision devices. Removal of the thin native oxide from Si surfaces in buffered HF prior to immersion in P-ED was also essential to ensure uniform etching and prevent hillock formation [36], [37]. Precipitates formed on Si surfaces after etching in P-ED were dissolved readily in buffered HF. P-ED was found to be stable and useful over periods of weeks provided the solution was kept in a nonoxidizing atmosphere and did not contain excessive amounts of Si. In a critical device application, etching control was best achieved with a fresh solution containing, if necessary, a higher percentage of ethylene diamine. The latter was required when occasional hillock formation persisted.

4

FABRICATION OF MICROSTRUCTURES

Nozzles

Arrays of nozzles of uniform size and spacing are required for the operation of ink jet printers using binary, deflected, electrostatically charged ink jets [38]-[41]. Two types of nozzles have been fabricated experimentally in (100) silicon which fulfill these requirements. The first is a pyramidal-shaped nozzle with a square orifice [16] which is formed by the anisotropic etching of holes through a (100) oriented Si wafer. The square orifice is defined by four convergent {111} planes which intersect the (100) surface of the wafer. In Fig. 4 examples are shown of discrete nozzles and arrays of nozzles with square orifices. The fabrication and performance of such devices in an experimental printer have been described elsewhere [18], [35]. The second type of nozzle is a circular orifice defined in a thin heavily doped p^+ Si membrane which is edge-supported in a pyramidal cavity etched in (100) Si [15].

Pyramidal-shaped holes for nozzle fabrication were etched in (100) Si wafers using patterns of different geometry. Openings in the SiO_2 film on the Si surface were square, circular, or open-cross, the last being a cross superimposed on a smaller square opening. The etched hole which was generated from a square opening was, as expected, identical in geometry to the opening itself provided it was aligned parallel to the $\langle 110 \rangle$ direction. A circular opening, however, yielded initially an octagonal-shaped hole in the Si surface. As etching pro-

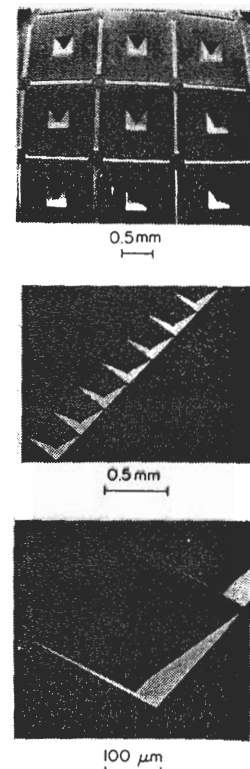


Fig. 4. SEM photomicrographs of ink jet printing nozzles etched in (100) silicon. (Top) 9 discrete nozzles on 1.2-mm centers on a silicon wafer. (Center) An array of 8 nozzles on 0.3-mm centers. (Bottom) Each nozzle is a truncated square pyramidal cavity $200 \mu\text{m}$ deep with an orifice $25 \times 25 \mu\text{m}^2$.

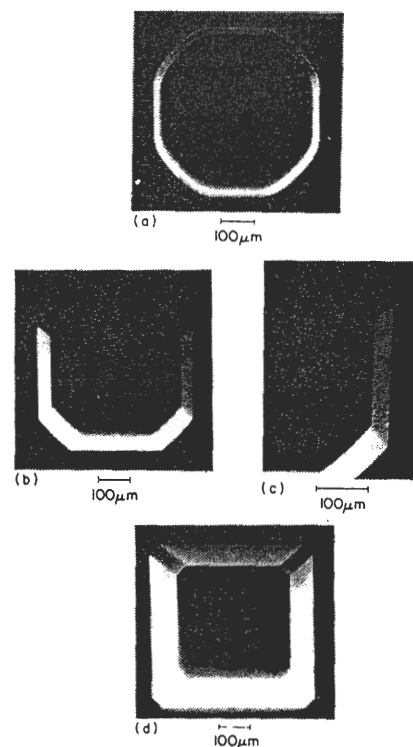


Fig. 5. SEM photomicrographs of a cavity etched progressively deeper into a (100) Si wafer through a circular opening in an SiO_2 surface film. Hole depth (a) $29 \mu\text{m}$; (b) $60 \mu\text{m}$; (c) a higher magnification of (b) showing multifaceted corners; (d) $120 \mu\text{m}$. Corners eventually disappear to form a square hole in the Si surface.

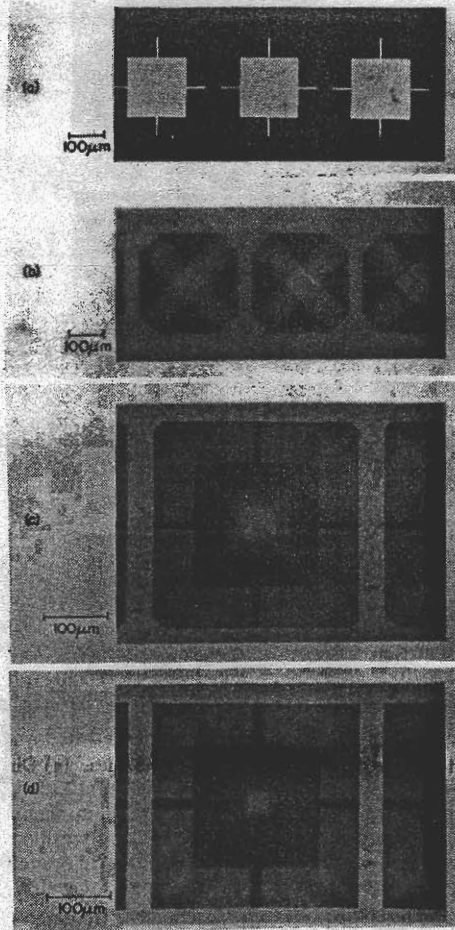


Fig. 6. Photomicrographs of an open-cross pattern etched progressively deeper into a (100) Si wafer through an SiO₂ etch mask. (a) Pattern geometry of three openings prior to etching. (b) Holes in silicon etched 120 μm deep. (c) Single hole etched 160 μm deep. (d) Hole 175 μm deep with a square base hole on the top surface and a square orifice etched through the opposite side of the wafer. The original surface pattern is clearly defined by the SiO₂ overhang.

gressed into the substrate, four well-defined {111} planes developed and increased in size until the octahedral hole became a square as shown in the SEM photomicrographs of Fig. 5. Close examination of Fig. 5(c) reveals that the corners of the octagon are multifaceted and not discrete crystallographic planes as was reported with other anisotropic etchants [26], [36]. An open-cross pattern exhibited a similar etching behavior with respect to the development of self-limiting {111} planes as shown in Fig. 6. This occurred due to the rapid etching of convex (mesa) corners under the oxide opening during the initial stages of etching. Fig. 7 is a SEM photomicrograph of a multifaceted cavity etched 30 μm deep into a (100) Si substrate using the open-cross pattern of Fig. 6. It illustrates convincingly the difference in stability of intersecting {111} planes at convex (mesa) and concave (cavity) corners and edges in P-ED etchant. With any of the patterns just described, the final geometry of the etched hole was the same after sufficient etching had occurred. As shown in Fig. 8, the dimensions of a square pyramidal hole is given by the expression

$$W_o = W_{Si} - \sqrt{2} t_{Si}$$

where W_o is the side of the square apex or orifice, W_{Si} the side

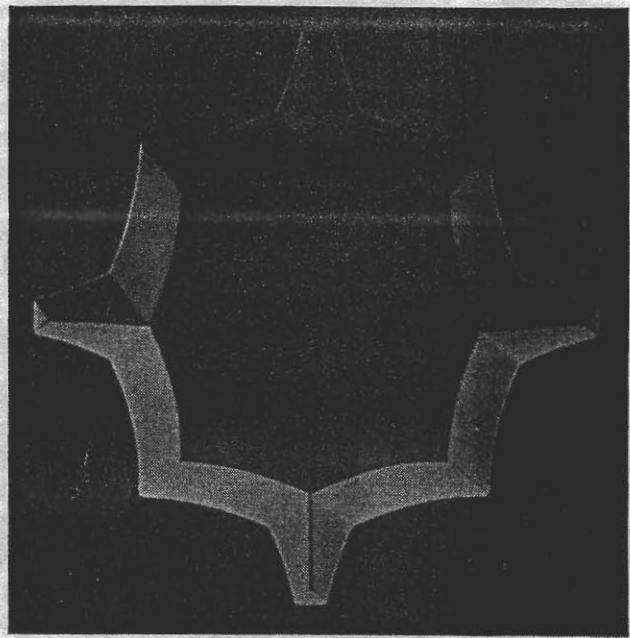


Fig. 7. SEM photomicrograph of an etched hole in a (100) Si surface using the open cross-pattern shown in Fig. 6. The oxide masking film is etched off to show the rapid etching and rounding of intersecting {111} planes at convex (mesa) corners and edges.

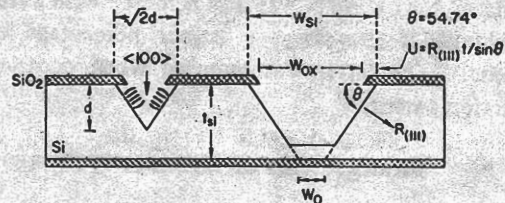


Fig. 8. Cross section through anisotropically etched pattern in (100) Si. The orifice dimension $W_o = W_{Si} - \sqrt{2} t_{Si}$, and the underetching U are a function of the etch rate $R_{(111)}$ of the {111} planes and etching time t for an accurately aligned pattern and a defect free Si-SiO₂ interface.

of the square base hole in the wafer surface, and t_{Si} the etched depth or wafer thickness. The underetching $U = R_{(111)}t / \sin \theta$ represents the difference between the oxide opening and the base hole in the Si surface. It is due to the small but finite etch rate of the {111} planes $R_{(111)}$, the etching time t , and the angle $\theta = 54.74^\circ$ between the {111} planes and (100) surface.

5 Membrane-type nozzles with circular orifices were fabricated by etching holes as previously described, in combination with a process which takes advantage of the etch resistance of heavily doped p⁺ Si in P-ED. At an impurity concentration $N_A \approx 10^{19} \text{ cm}^{-3}$ the etch rate of Si in P-ED drops sharply and reaches practically zero at $N_A \geq 7 \times 10^{19} \text{ cm}^{-3}$ [42], [43]. When a silicon wafer with a heavily doped p⁺ surface layer is etched in P-ED, the undoped Si is removed and a membrane is left whose thickness is equal to the depth of the surface layer with a concentration $N_A \geq 7 \times 10^{19} \text{ cm}^{-3}$. This property has been used to fabricate various device structures incorporating membranes ranging in thickness between 1 and 10 μm [1]-[5], [20], [21], [28]. This technique was also used to fabricate a high-precision orifice in a p⁺ Si membrane for use as an ink jet printing nozzle. The fabrication process of this membrane

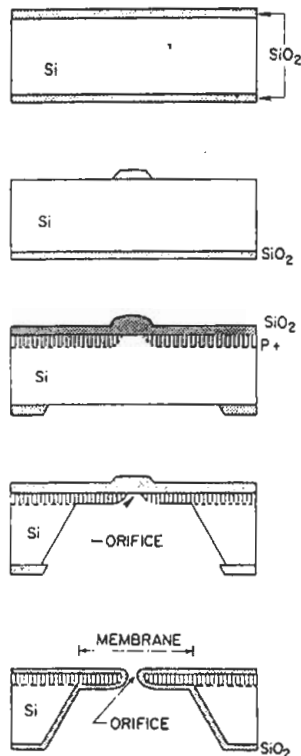


Fig. 9. Method of fabricating a silicon membrane nozzle using conventional processing techniques. The nozzle is a high-precision orifice defined in a thin heavily doped p^+ Si membrane. A (100) Si wafer is oxidized; an orifice pattern is defined on one side of the wafer followed by a heavy p^+ (boron) diffusion, reoxidation, and opening of a base hole in the SiO_2 film on the opposite side. Anisotropic etching through the wafer proceeds along the $\{111\}$ planes and the contour of the p^+ diffusion profile; finally, the SiO_2 masking film is stripped off and the wafer reoxidized.

nozzle is illustrated schematically in Fig. 9. A clean Si wafer of (100) orientation, chem-mechanically polished on both sides, either p- or n-type, $0.1\text{--}20\ \Omega\cdot\text{cm}$ was thermally oxidized to grow an SiO_2 film $1\text{--}2\ \mu\text{m}$ thick. This film served as a boron diffusion mask in the subsequent processing step. A thinner masking layer was sometimes employed by replacing the SiO_2 film with a dual layer of $\text{SiO}_2 + \text{Si}_3\text{N}_4$. An orifice pattern consisting of an array of circular SiO_2 dots was delineated photolithographically on one side of the wafer while protecting the SiO_2 layer on the opposite side. Each SiO_2 dot defined the geometry of the orifice in the final structure. A boron diffusion from a BBr_3 source was then carried out under conditions which resulted in a boron surface concentration close to its solubility limit in silicon. The thickness of the p^+ Si membrane in the final structure was equal to the region in the p^+ surface layer whose concentration $N_A \geq 7 \times 10^{19}\ \text{cm}^{-3}$. In $10\text{-}\Omega\cdot\text{cm}$ Si, a junction depth $8\ \mu\text{m}$ deep, yielded a membrane approximately $3\ \mu\text{m}$ thick. After diffusion, an SiO_2 film approximately $1\ \mu\text{m}$ thick was thermally grown on the doped surface. A base hole pattern was delineated photolithographically on the other side of the wafer, and pyramidal holes were then etched through the substrate to form orifices in a membrane on the diffused side of the wafer. Excessive etching had no effect either on the p^+ Si membrane or on the size of the orifice, but the base hole increased slightly in size due to the small etch rate of the $\{111\}$ sidewalls. As shown in Fig. 9, the orifice geometry is defined by the masked region on the

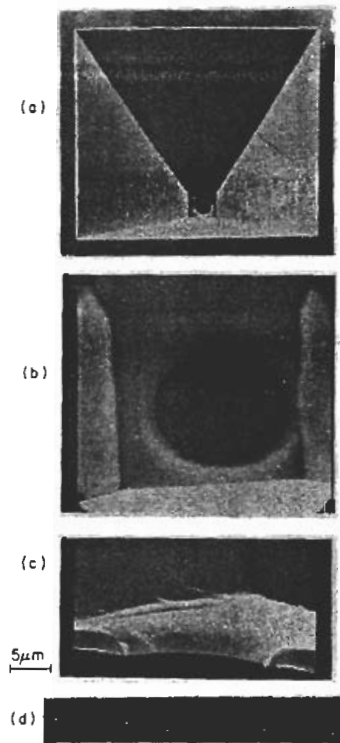


Fig. 10. Photomicrographs of Si membrane nozzles. (a) Discrete nozzle looking down the square base hole $0.4 \times 0.4\ \text{mm}^2$ of the pyramidal cavity $0.2\ \text{mm}$ deep. (b) Circular orifice $\sim 20\text{-}\mu\text{m}$ diameter in a rectangular p^+ Si membrane $3\ \mu\text{m}$ thick. (c) Cross section of an orifice showing the flared contour of the edge. (d) Five discrete nozzles on 0.6-mm centers viewed from the orifice side of the wafer.

wafer surface and by the boron diffusion junction. After P-ED etching was completed, the oxide layers on the front and back surfaces were stripped off, and a uniform SiO_2 film $\sim 1\ \mu\text{m}$ thick was thermally grown on all exposed Si surfaces of the nozzle. In the fabrication process, the registration of the orifice and base hole patterns and their respective alignment to the wafer's crystal axes were accomplished by the help of holes etched through the wafer prior to pattern definition. For more moderate registration accuracy, alignment features on the photomask, and mechanical adjustments on the optical exposure system were adequate. Nozzles with an orifice diameter $\sim 20\ \mu\text{m}$, in a p^+ Si membrane $3\ \mu\text{m}$ thick are shown in Fig. 10. The flared contour of the orifice edge, which is apparent in a cross section of the orifice, results from the boron diffusion profile under the edge of the SiO_2 orifice mask.

The geometry of the orifice in membrane nozzles is not restricted to circular openings but can be controlled by orifice pattern design and by the diffusion conditions. Orifice dimensions can be increased in small increments by isotropic etching or by oxidation and oxide stripping. Orifice dimensions in the submicrometer range using optically defined patterns are feasible by adjusting the diffusion time and thereby the lateral spread of the dopant under the orifice diffusion mask. Finally, multiple orifices on the same membrane formed on (100) and (110) Si could be fabricated as shown in Fig. 11.

(6) Multisocket Electrical Connector

A miniature electrical connector for packaging electronic circuits which are required to operate at cryogenic temperatures, was fabricated by bonding two wafers possessing

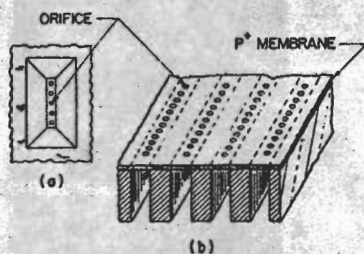


Fig. 11. Multiple orifices in a single p^+ Si membrane on (a) (100) Si wafer, and (b) (110) Si wafer using the fabrication method outlined in Fig. 9.

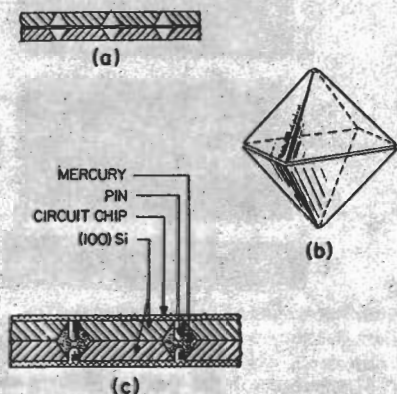


Fig. 12. Multisocket electrical connector for packaging cryogenic circuits is formed by bonding two identical wafers in which are etched pyramidal cavities. (a) Cross section of three cavities. (b) Each cavity is an octahedral structure formed of two nozzles with square orifices of the type shown in Fig. 4. (c) Mercury in the cavities serves as the electrically conductive medium in the final packaged circuits.

identical arrays of truncated pyramidal holes [44]. The resulting structure consisted of arrays of octahedral cavities with small square openings $125 \times 125 \mu\text{m}^2$ on opposite sides of the laminated wafers as shown in Fig. 12. In operation, the cavities are filled with a suitable, low-melting, conducting material such as mercury, which is retained inside the cavities at room temperature due to surface tension. Input and output signals from individual circuit elements are carried via pins which are inserted from opposite sides of the connector as shown in Fig. 12. The zero insertion force of this high-density demountable connector is one of its major attributes.

The fabrication of the connector employed the same techniques used for fabricating nozzles. Two identically processed silicon wafers with mirror-image nozzle array patterns were aligned and bonded with their base hole sides in contact to form the required octahedral cavities. The bonding process is a novel technique which takes advantage of the relatively low melting point of phosphosilicate glass (PSG) films, and of the ease with which thin uniform layers of PSG are formed on oxidized Si surfaces. After the nozzles were etched, the SiO_2 film which served as an etching mask was stripped off, and a new SiO_2 film 1–2 μm thick was then thermally grown on the wafers. A PSG layer containing approximately 10 percent P_2O_5 was formed on the SiO_2 surfaces by exposing the wafers to a mixture of phosphorus oxychloride POCl_3 vapor and O_2 gas at 900°C . The wafers were then aligned and clamped together inside a quartz vacuum-chuck assembly which forced the wafer surfaces into intimate contact by connecting it to a vacuum pump throughout the bonding process. The quartz

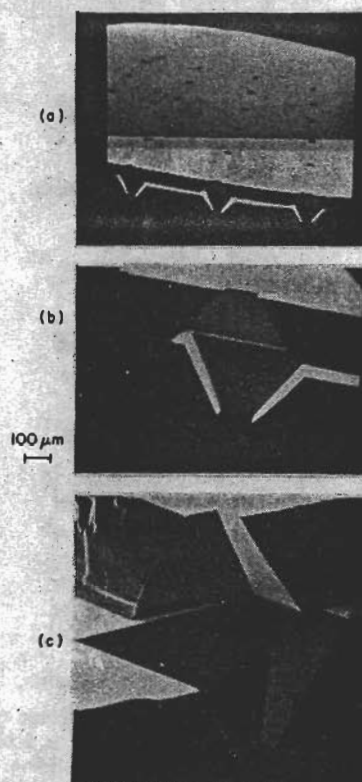


Fig. 13. SEM photomicrographs of a multisocket electrical connector. The cavities are on 1.3-mm centers, overall height 0.6 mm, square openings on opposite sides are $125 \times 125 \mu\text{m}^2$, opening at the center $0.45 \times 0.45 \text{mm}^2$. (a) Bonded, completed structure. (b) Cross section of an octahedral cavity. (c) Cross section showing $\{111\}$ sidewalls of the upper and lower parts of the same cavity.

assembly was introduced into a furnace at 1100°C and heated for 30 min, then slowly cooled to room temperature. Fusion of the PSG layers took place readily and the resulting bond strength was excellent provided the wafer surfaces were clean and reasonably flat. The completed bonded structure is shown in Fig. 13. Electrical connectors made by this process were cycled repeatedly between liquid nitrogen and room temperature without suffering structural failures.

Multichannel Arrays

Arrays of parallel trenches and channels with V-shaped and U-shaped cross sections, as shown in Fig. 14, were fabricated by etching long rectangular openings in (100) and (110) Si, respectively. Control of channel width and spacing was critically dependent on accurate wafer orientation and pattern alignment as well as on the use of defect free substrates. Misalignment generated sidewall imperfections and caused merging between adjacent channels especially in long dense structures. The nature of the imperfections in the sidewalls of vertically etched grooves in (110) Si has been discussed by Kendall [14]. The arrays of V-shaped trenches shown in Fig. 14(a) and (b) were used in making optical waveguides [8]. The structure shown in Fig. 14(c) consists of eight equally spaced rectangular slots 200 μm wide with vertical sidewalls etched in a (110) Si wafer 200 μm thick. Structures such as this, have been used as charge electrodes in ink jet printing [45], as physical masks for evaporation and reactive ion etching, and in the fabrication of a multiprobe electrical connector for use at cryogenic temperatures. The latter was fabricated by sawing symmetrically

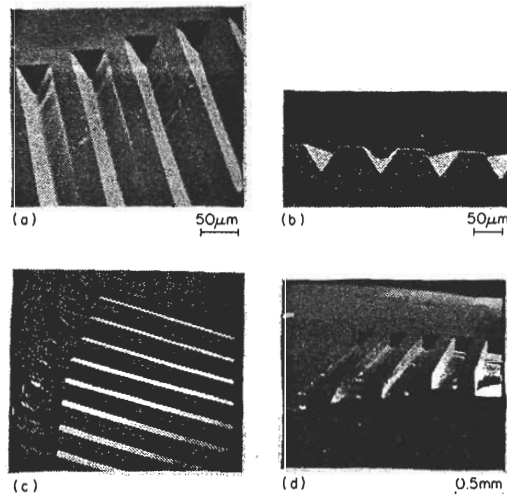


Fig. 14. Anisotropically etched channels in single crystal silicon. (a) (100) orientation. (b) Cross section of (a). (c) Bars and slots 200 μm wide with vertical sidewalls etched through a (110) Si wafer 200 μm thick. (d) Parallel trenches etched in (110) Si.

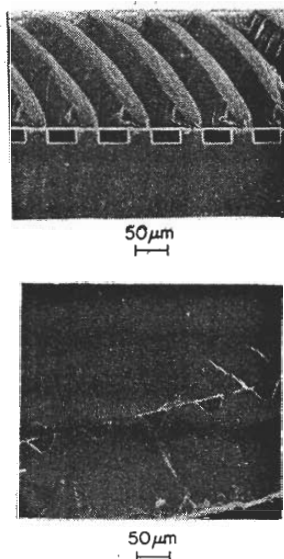


Fig. 15. Cross sections of enclosed arrays of channels formed by fusing the surfaces of two silicon wafers with phosphosilicate glass films. One surface is planar and the other surface has parallel trenches etched in a (110) Si wafer (top) and a (100) Si wafer (bottom).

across an array of slots, forming thereby, two identical in-line, multiple probe structures. Electrically conducting regions were formed by conventional diffusion and metallization techniques. Using the PSG bonding method described above, enclosed channel structures were also fabricated by laminating pairs of etched and planar silicon wafers. Cross sections obtained by cleaving such structures are shown in Fig. 15.

In conclusion, the three-dimensional microstructures described in this paper are bulk and surface structured devices whose geometry is dictated by the crystallography of the silicon substrate and the anisotropic etching characteristics of P-ED solutions. The self-limiting geometry is an advantage in fabricating predictable device structures with a high degree of precision. Where such a limitation is too restrictive, anisotropic and isotropic etching techniques could be used in combination to extend the range of device geometry. The use of thin silicon

wafers also limits the geometry to structures which can be fabricated by processing the two surfaces of the substrate. Such a limitation is not inherent in the crystal structure of the substrate itself; in fact, the cubic symmetry of single-crystal silicon makes it a natural candidate for the fabrication of three-dimensional microstructures in a polyhedral substrate. The bonding technique which utilizes thin PSG films to fuse silicon wafers is also applicable to silicon-coated substrates and to silicate glasses which are capable of withstanding elevated temperatures. By fusing several discrete components made from these materials, complex, multifunctional, three-dimensional structures could be fabricated.

ACKNOWLEDGMENT

The author wishes to thank A. Reisman, C. M. Osburn, L. Kuhn, H. N. Yu, and K. C. Park for helpful discussions and support of this work. The technical assistance of H. F. Lazzari, E. F. Baran, J. Wilson, J. A. Kucza, V. Maniscalco, M. J. Smyth, A. Cramer, and E. J. Petrillo is gratefully acknowledged. Thanks are due to W. D. Grobman for the photomask used in Fig. 6.

REFERENCES

- [1] D. L. Spears and H. I. Smith, "X-ray lithography: A new high resolution replication process," *Solid State Technol.*, vol. 15, pp. 21-26, July 1972.
- [2] D. L. Spears and H. I. Smith, "High resolution pattern replication using soft x-rays," *Electron Lett.*, vol. 8, no. 4, pp. 102-104, Feb. 24, 1972.
- [3] D. L. Spears, H. I. Smith, and E. Stern, "X-ray replication scanning electron microscope generated patterns," in *Proc. 5th Int. Conf. Electron and Ion Beams in Science and Technology*, R. Bakish, Ed. Princeton, NJ: The Electrochemical Society, p. 80.
- [4] C. J. Schmidt, P. V. Lenzo, and E. G. Spencer, "Preparation of thin windows in silicon masks for X-ray lithography," *J. Appl. Phys.*, vol. 46, no. 9, pp. 4080-4082, Sept. 1975.
- [5] P. V. Lenzo and E. G. Spencer, "High-speed low-power x-ray lithography," *Appl. Phys. Lett.*, vol. 24, no. 6, pp. 289-291, Mar. 1974.
- [6] E. Bassous, R. Feder, E. Spiller, and J. Topalian, "High transmission X-ray masks for lithographic applications," *Solid State Technol.*, vol. 19, no. 9, pp. 55-58, Sept. 1976.
- [7] W. T. Tsang, C. C. Tseng, and S. Wang, "Optical waveguides fabricated by preferential etching," *Appl. Opt.*, vol. 14, no. 5, pp. 1200-1206, May 1975.
- [8] J. S. Harper and P. F. Heidrich, "High density multichannel optical waveguides with integrated couplers," *Wave Electronics*, vol. 2, pp. 369-377, 1976.
- [9] J. D. Crow, L. D. Comerford, R. A. Laff, M. J. Brady, and J. S. Harper, "GaAs laser array source package," *Opt. Lett.*, vol. 1, no. 1, pp. 40-42, July 1977.
- [10] T. O. Sedgwick, A. N. Broers, and B. J. Agule, "A novel method for fabrication of ultrafine metal lines by electron beams," *J. Electrochem. Soc.*, vol. 119, no. 12, pp. 1769-1771, Dec. 1972.
- [11] W. K. Zwicker, "Method of producing high resolution patterns in single crystals," U.S. Patent 3 770 533, Nov. 1973.
- [12] A. I. Stoller, "The etching of deep vertical-walled patterns in silicon," *RCA Rev.*, vol. 31, pp. 271-275, June 1970.
- [13] W. T. Tsang and S. Wang, "Preferentially etched diffraction gratings in silicon," *J. Appl. Phys.*, vol. 46, no. 5, pp. 2163-2166, May 1975.
- [14] D. L. Kendall, "On etching very narrow grooves in silicon," *Appl. Phys. Lett.*, vol. 26, pp. 1500-1503, Nov. 1974.
- [15] E. Bassous, "Nozzles formed in monocrystalline silicon," U.S. Patent 3 921 916, Nov. 1975.
- [16] E. Bassous, L. Kuhn, A. Reisman, and H. H. Taub, "Ink jet nozzle," U.S. Patent 4 007 464, Feb. 1977.
- [17] C. Chiou, K. H. Loeffler, and M. R. Lorenz, "Ink jet nozzle structure," U.S. Patent 3 958 255, May 1976.

- [18] E. Bassous, H. H. Taub, and L. Kuhn "Ink jet printing nozzle arrays etched in silicon," *Appl. Phys. Lett.*, vol. 31, no. 2, pp. 135-137, July 1977.
- [19] D. A. Kiewit, "Microtool fabrication by etch pit replication," *Rev. Sci. Instrum.*, vol. 44, no. 12, pp. 1741-1742, Dec. 1973.
- [20] C. L. Huang and T. Van Duzer, "Schottky diodes and other devices on thin silicon membranes," *IEEE Trans. Electron Devices*, vol. ED-23, no. 6, pp. 579-583, June 1976.
- [21] —, "Josephson tunneling through locally thinned silicon wafers," *Appl. Phys. Lett.*, vol. 25, no. 12, pp. 753-756, Dec. 1974.
- [22] T. J. Rodgers and J. D. Meindl, "Epitaxial V-groove bipolar integrated circuit process," *IEEE Trans. Electron Devices*, vol. ED-20, pp. 226-232, Mar. 1973.
- [23] T. J. Rodgers and J. D. Meindl, "VMOS: High speed TTL compatible MOS logic," *IEEE J. Solid-State Circuits*, vol. SC-9, pp. 239-249, Oct. 1974.
- [24] M. J. Declercq, "A new C-MOS technology using anisotropic etching of silicon," *IEEE J. Solid-State Circuits*, vol. SC-10, no. 4, pp. 191-197, Aug. 1975.
- [25] P. Ou-Yang, "Double ion implanted V-MOS technology," *IEEE J. Solid-State Circuits*, vol. SC-12, no. 1, pp. 3-10, Feb. 1977.
- [26] K. E. Bean and J. R. Lawson, "Application of silicon crystal orientation and anisotropic effects to the control of charge spreading in devices," *IEEE J. Solid-State Circuits*, vol. SC-9, no. 3, pp. 111-117, June 1974.
- [27] K. E. Bean and W. R. Runyan "Dielectric isolation: comprehensive, current and future," *J. Electrochem. Soc.*, vol. 124, no. 1, pp. SC-12C, Jan. 1977.
- ✓ [28] H. Guckel, S. Larsen, M. G. Lagally, G. Moore, J. B. Miller, and J. D. Wiley, "Electromechanical devices utilizing thin Si diaphragms," *Appl. Phys. Lett.*, vol. 31, no. 9, pp. 618-619, Nov. 1977.
- ✓ [29] S. C. Terry, "A gas chromatography system fabricated on a silicon wafer using integrated circuit technology," Ph.D. dissertation, Stanford Univ. Elec. Eng. Dept., 1975.
- ✓ [30] K. E. Peterson, "Micromechanical light modulator array fabricated on silicon," *Appl. Phys. Lett.*, vol. 31, no. 8, pp. 521-523, Oct. 1977.
- [31] H. C. Nathanson and J. Guldberg, "Topologically structured thin films in semiconductor device operation," in *Physics of Thin Films*, vol. 8, G. Hass, M. H. Francombe, and R. W. Hoffman, Eds. New York: Academic Press, pp. 251-333.
- [32] H. C. Nathanson, "New directions in nonplanar semiconductor device technology," in *IEDM Tech. Dig.*, pp. 4-8, 1976.
- [33] R. N. Thomas, J. Guldberg, H. C. Nathanson, and P. R. Malmberg, "The mirror matrix tube: A novel light valve for projection displays," *IEEE Trans. Electron Devices*, vol. ED-22, no. 9, pp. 765-775, Sept. 1975.
- [34] R. M. Finne and D. L. Klein "A water-amine-complexing agent system for etching silicon," *J. Electrochem. Soc.*, vol. 114, pp. 965-970, Sept. 1967.
- [35] E. Bassous and E. F. Baran, "Fabrication of silicon nozzle arrays for ink jet printing," presented at the Electrochemical Society Fall Meeting, Atlanta, GA, Oct. 1977; also in *Extended Abstracts*, vol. 77-2, pp. 954-955, 1977.
- [36] D. B. Lee, "Anisotropic etching of silicon," *J. Appl. Phys.*, vol. 40, no. 11, pp. 4569-4574, Oct. 1969.
- [37] M. J. Declercq, L. Gerzberg, and J. D. Meindl, "Optimization of of hydrazine-water solution for anisotropic etching of silicon in integrated circuit technology," *J. Electrochem. Soc.*, vol. 122, no. 4, pp. 545-552, Apr. 1975.
- [38] R. G. Sweet, "High frequency recording with electrostatically deflected ink jets," *Rev. Sci. Instrum.*, vol. 36, no. 2, pp. 131-136, Feb. 1965.
- [39] R. G. Sweet, "Fluid droplet recorder," U.S. Patent 3 596 275, Jul. 1971.
- ✓ [40] F. J. Kamphoefner, "Ink jet printing," *IEEE Trans. Electron Devices*, vol. ED-19, no. 4, pp. 584-593, Apr. 1972.
- ✓ [41] R. D. Carnahan and S. L. Hou, "Ink jet technology," *IEEE Trans. Ind. App.*, vol. IA-13, no. 1, pp. 95-105, Jan./Feb. 1977.
- [42] J. C. Greenwood, "Ethylene diamine-catechol-water mixture shows preferential etching of p-n junction," *J. Electrochem. Soc.*, vol. 116, no. 9, pp. 1325-1326, Sept. 1969.
- [43] A. Bohg, "Ethylene diamine-pyrocatechol-water mixture shows etching anomaly in boron-doped silicon," *J. Electrochem. Soc.*, vol. 118, no. 2, pp. 401-402, Feb. 1971.
- [44] W. Anacker, E. Bassous, F. F. Fang, R. E. Mundie, and H. N. Yu, "Fabrication of multiprobe miniature electrical connector," *IBM Tech. Discl. Bull.*, vol. 19, no. 1, pp. 372-374, June 1976.
- [45] E. Bassous and L. Kuhn, "Charge electrode array and combination for ink jet printing and method of manufacture," U.S. Patent 4 047 184, Sept. 1977.

Anisotropic Etching of Silicon

KENNETH E. BEAN

Abstract—Anisotropic etching of silicon has become an important technology in silicon semiconductor processing during the past ten years. It will continue to gain stature and acceptance as standard processing technology in the next few years. Anisotropic etching of (100) orientation silicon is being widely used today and (110) orientation technology is emerging. This paper discusses both orientation-dependent and concentration-dependent etching of (100) and (110) silicon. Very exact process control steps may be designed into a process by use of (100) anisotropic and concentration-dependent etching. Also, methods of oxide or nitride pin hole detection in (100) silicon are pre-

sented. Mask alignments to obtain different etch front termination in both (100) and (110) silicon are shown. Very high packing density structures, less than 1 μm , are obtained in the (110) technology, and extremely high etching ratios of greater than 650 to 1 are obtained in (110) orientation-dependent etching. Some of the many applications for anisotropic and concentration-dependent etching are described.

ORIENTATION-DEPENDENT ETCHING

WET CHEMICAL ETCHING has been used in silicon semiconductor processing since its beginning in the early 1950's. Isotropic etches, i.e., etches that etch in all crystallographic direction at the same rate, consisting of hydro-

Manuscript received March 16, 1978; revised June 26, 1978.
The author is with Texas Instruments, Inc., Central Research Laboratory, Dallas, TX 75222.